

RECLAMATION

Managing Water in the West

Technical Publication No. 8540-2019-03

Electrochemical Impedance Methods to Assess Coatings for Corrosion Protection



U.S. Department of the Interior
Bureau of Reclamation
Technical Service Center
Materials and Corrosion Laboratory
Denver, Colorado

January 2019

Mission Statements

Protecting America's Great Outdoors and Powering Our Future

The Department of the Interior protects and manages the Nation's natural resources and cultural heritage; provides scientific and other information about those resources; and honors its trust responsibilities or special commitments to American Indians, Alaska Natives, and affiliated island communities.

Cover photo: Field EIS data collection within siphon pipe.

Disclaimer:

This document has been reviewed consistent with the Bureau of Reclamation's (Reclamation) Peer Review Policy CMP P14. It does not represent and should not be construed to represent Reclamation's determination, concurrence, or policy.

REPORT DOCUMENTATION PAGE			Form Approved OMB No. 0704-0188		
T1. REPORT DATE: January 2019		T2. REPORT TYPE: Technical Guidance		T3. DATES COVERED November 2014 to January 2019	
T4. TITLE AND SUBTITLE Electrochemical Impedance Methods to Assess Coatings for Corrosion Protection			5a. CONTRACT NUMBER 190R5065C6-RX596898701120101		
			5b. GRANT NUMBER N/A		
			5c. PROGRAM ELEMENT NUMBER		
6. AUTHOR(S) Bobbi Jo E. Merten, bmerten@usbr.gov, 303-445-2380			5d. PROJECT NUMBER		
			5e. TASK NUMBER		
			5f. WORK UNIT NUMBER 86-68540		
7. PERFORMING ORGANIZATION NAME(S) AND ADDRESS(ES) Bobbi Jo E. Merten Technical Service Center, Materials and Corrosion Laboratory, U.S. Department of the Interior, Bureau of Reclamation, PO Box 25007, Denver CO 80225-0007			8. PERFORMING ORGANIZATION REPORT NUMBER 8540-2019-03		
9. SPONSORING / MONITORING AGENCY NAME(S) AND ADDRESS(ES) U.S. Department of the Interior, Bureau of Reclamation, PO Box 25007, Denver CO 80225-0007			10. SPONSOR/MONITOR'S ACRONYM(S) R&D: Research and Development Office BOR/USBR: Bureau of Reclamation DOI: Department of the Interior		
			11. SPONSOR/MONITOR'S REPORT NUMBER(S)		
12. DISTRIBUTION / AVAILABILITY STATEMENT Contact organization for a copy of the technical publication.					
13. SUPPLEMENTARY NOTES					
14. ABSTRACT: Electrochemical impedance spectroscopy (EIS) allows for a quantitative analysis of protective coatings, whether testing new coatings in the lab or evaluating aged coating on Reclamation's structures. EIS data increases the robustness of any assessment. This technical publication explains the fundamentals of EIS, provides approaches for analyzing the data, and includes laboratory and field test methods to guide the laboratory or field engineer in producing successful EIS tests.					
15. SUBJECT TERMS: Electrochemical impedance spectroscopy, field EIS, coating assessment, impedance analysis, coatings, corrosion protection, quantitative assessment, coating service life					
16. SECURITY CLASSIFICATION OF:			17. LIMITATION OF ABSTRACT	18. NUMBER OF PAGES	19a. NAME OF RESPONSIBLE PERSON
a. REPORT	b. ABSTRACT	c. THIS PAGE	U	45	Bobbi Jo Merten
U	U	U			19b. TELEPHONE NUMBER 303-445-2380

BUREAU OF RECLAMATION

**Technical Service Center, Denver, Colorado
Materials and Corrosion Laboratory, 86-68540
Technical Publication No. 8540-2019-03**

Electrochemical Impedance Methods to Assess Coatings for Corrosion Protection

Prepared by: Bobbi Jo Merten, Ph.D.
Coatings Specialist, Materials and Corrosion Laboratory, 86-68540

Checked by: Stephanie Prochaska
Materials Engineer, Materials and Corrosion Laboratory, 86-68540

Technical Approval: Chrissy Henderson
Materials Engineer, Materials and Corrosion Laboratory, 86-68540

Peer Review: Allen Skaja, Ph.D.
Coatings Specialist, Materials and Corrosion Laboratory, 86-68540

Peer Review: David Tordonato, Ph.D., PE
Materials Engineer, Materials and Corrosion Laboratory, 86-68540

Acknowledgements

The authors are grateful for funding provided by the Bureau of Reclamation's Manuals and Standards and Science and Technology Programs. The authors also acknowledge the following facilities for field electrochemical impedance spectroscopy demonstrations or method incorporation into scheduled coating assessments: Wilbur Mills Lock and Dam, Ozark Lock and Dam, Green Springs Powerplant, Dworshak Dam, Little Oso Dam, Marston Water Treatment Plant, Green Mountain Powerplant, Boysen Dam, Glen Canyon Powerplant, Grand Coulee Powerplant, Agua Fria Siphon, and Salt River Siphon.

Acronyms and Abbreviations

AC	alternating current
CDL	coating double layer capacitance
CE	counter electrode
cm	centimeter
cm ²	square centimeter
CPE	constant phase element
CSE	copper-copper sulfate electrode
DC	direct current
DHS	dilute Harrison's solution
ECM	equivalent circuit modeling
EIS	electrochemical impedance spectroscopy
EPA	Environmental Protection Agency
F	Farads
ft ²	square foot
Freq.	frequency
Hz	Hertz
mL	milliliters
mV	millivolts
NaCl	sodium chloride
(NH ₄) ₂ SO ₄	ammonium sulfate
OCP	open circuit potential
PPE	personal protective equipment
Pt	platinum
PVC	polyvinyl chloride

RE	reference electrode
SCE	saturated calomel electrode
sec	second
SSCE	silver-silver chloride electrode
VOC	volatile organic compound
WE	working electrode
wt. %	weight percent

Symbols

A	area
b_a	anodic Tafel slope
b_c	cathodic Tafel slope
C_c	coating capacitance
C_{dl}	double layer capacitance
CPE_{coat}	coating constant phase element
d	distance
E	potential
f	frequency
I	current
i_{corr}	corrosion rate
j	imaginary number, $\sqrt{-1}$
R	resistance
R_p	polarization resistance
R_{pore}	pore resistance
R_s	solution resistance

R_{ct}	charge transfer resistance
t	time
V	voltage
Z	impedance
Z_{real}	real impedance
Z_{imag}	imaginary impedance
$ Z $	impedance magnitude
$ Z _{0.01\text{ Hz}}$	impedance magnitude at 0.01 Hz
$ Z _{0.05\text{ Hz}}$	impedance magnitude at 0.05 Hz
α	constant phase element exponent
Δ	delta
ε	permittivity (dielectric constant)
ε_0	permittivity of a vacuum
θ	phase angle
ρ	resistivity
ω	angular frequency
Ω	ohms
∞	infinity

Contents

	Page
1. Introduction.....	1
1.1. Maintenance of Coated Structures.....	1
2. Fundamentals of EIS.....	2
2.1. Underlying Principals.....	2
2.2. Measurement Parameters.....	5
2.3. Raw Data Presentation and Interpretation.....	6
3. Analysis of EIS Data Sets.....	9
3.1. Coating Sampling (Estimating Coating Quality).....	9
3.1.1. Low Frequency Impedance.....	10
3.1.2. Probability Plot.....	11
3.2. Longitudinal Analysis (Estimating Service Life).....	12
3.3. Deriving Material Properties.....	13
3.3.1. Equivalent Circuit Modeling of Coatings.....	14
3.3.2. Physical Material Properties.....	17
4. EIS Measurement Procedures.....	18
4.1. Laboratory EIS Testing.....	18
4.1.1. Materials.....	18
4.1.2. Method.....	19
4.2. Field EIS Coating Inspection.....	23
4.2.1. Materials.....	23
4.2.1. Method.....	23
5. References.....	26

Tables

	Page
Table 1. Impedance relationships for circuit resistances and capacitances.	3
Table 2. Equipment items for laboratory EIS testing	19
Table 3. Recommended EIS parameters and inputs	21
Table 4. Equipment items for one field EIS test cell setup.....	23
Table 5. Recommended field EIS parameters and inputs.	25

Figures

	Page
Figure 1. Schematic of sinusoidal applied voltage and current response as a function of time for EIS measurements.	3
Figure 2. Parallel resistor-capacitor for three inputs of R and C.....	4
Figure 3. Schematic polarization curve with approximate EIS analysis location (linear region) identified.	6
Figure 4. EIS data presented by (a) Nyquist plot and (b) Bode plot.....	7
Figure 5. Schematic curves for two time constants, Warburg diffusion, and inductance as (a) Nyquist and (b) Bode plots (impedance magnitude only).	8
Figure 6. Impedance magnitude at 0.05 Hz versus pipe segment; corresponding elevations inset.....	10
Figure 7. Probability plot of low frequency impedance data (reproduced from [29]).....	11
Figure 8. Low frequency EIS data versus time of exposure.	13
Figure 9. ECM fitting results for a simple Randles cell by (left) Nyquist and (right) Bode plots.	15
Figure 10. ECM fitting results resistor-capacitor revised with constant phase element by (left) Nyquist and (right) Bode plots.	16
Figure 11. Coating equivalent circuit model with traditional circuit elements.....	17
Figure 12. Test cell set-up within Faraday cage for EIS.....	21
Figure 13. Screenshot of potentiostatic EIS typical test parameters and inputs. ...	22
Figure 14. Screenshot of completed EIS test Bode plot showing phase angle (top) and impedance magnitude (bottom).....	22
Figure 15. Attachment of EIS test cells to clean, dry, and defect-free coating surface.	25
Figure 16. Field EIS test (left) overview of setup and (right) detail of test cells and electrodes.....	25

1. Introduction

Coating specialists conduct laboratory evaluations of coatings used in Reclamation's guide specifications to evaluate manufacturer's products and provide quality assurance. The evaluations include a wide range of qualitative and quantitative analysis techniques, including electrochemical impedance spectroscopy (EIS). The Materials and Corrosion Laboratory, previously the Materials Engineering Research Laboratory, initiated EIS analysis in 2006.

EIS measurement and analysis procedures are presented in this guide as a tool for both materials selection and condition assessment of coatings. The advantages gained by performing EIS include:

- Quantitative material evaluation of new and modified commercial products.
- Quality assurance testing to confirm that an applied coating system conforms to specifications.
- Failure analysis of underperforming coatings.
- Coated infrastructure assessment to estimate remaining service life, improve maintenance scheduling, and reduce coating lifecycle costs.

This guide outlines practices for use of EIS to augment visual analysis. It begins with EIS fundamentals and then focuses on procedures for plotting and analyzing the data. This includes equivalent circuit modeling and the extraction of physical properties. The second half of the guide provides detailed descriptions of laboratory and field inspection methods.

1.1. Maintenance of Coated Structures

The protective coatings technologies applied to Reclamation infrastructure were commensurate with standard practices at the time. Many of the original coal tar- and lead-based products remain in service today, demonstrating service lifetimes consistently exceeding 50 years. For example, the coal tar enamel penstock interior coatings, i.e. linings, at Hoover Dam are in fair condition following more than 80 years of immersion service and several rounds of spot repair. However, the original coating systems are no longer feasible to apply due to work safety and health risks, including toxic fumes and solvents and volatile organic compound (VOC) limits exceeding current Environmental Protection Agency (EPA) regulations.

The frequency of coating maintenance activities at Reclamation facilities is increasing. The long service life coating systems will eventually need to be completely removed and the structure recoated with an alternative material. Ideally, this occurs when the coating completes its full lifecycle but before significant metal loss of the structure occurs. Challenges associated with planning for infrastructure recoating include:

- **Regulatory Compliance.** Environmental regulations limit today's use of historical products, including coal tar- and lead-based coatings. Occupational safety and health regulations dictate extensive measures to protect workers performing coating activities, particularly in confined spaces.

- **Construction Costs.** All aspects of construction costs (materials, labor, regulatory compliance, etc.) continue to increase. Contracting companies must be able to develop safe work plans to meet the scope of work with limited accessibility and short contract periods. Contract modifications are common due to unknown or unanticipated site or project conditions.
- **New Coating Materials.** Epoxies, polyurethanes, and other synthetic coating technologies entered the protective coatings market after World War II. These materials generally achieve present regulatory compliance but at a reduced service lifetime.
- **Operational Commitments.** Demand for reliable water delivery continues to increase as customer populations grow. Coatings must protect infrastructure assets at minimal cost and minimal interruption of service to end users.

The most economical solution to these challenges is to extend coating maintenance schedules without incurring metal loss to the structure. The following practices may help to optimize costs: 1) delay the recoating to maximize the existing coating service life (although without incurring costly structure metal loss), and 2) select a replacement material with the longest service life and ensure the highest quality surface preparation and application.

2. Fundamentals of EIS

Bacon, et al. provided one of the earliest EIS precursor evaluations, measuring the direct current (DC) resistance of more than 500 coating materials on metal substrates [1]. The DC measurements led to the development and use of alternating current (AC) signals, which allowed the experimenter to measure resistive and capacitive changes to a coating following exposure to a degrading environment; this AC evaluation is the basis of EIS. Equipment improvements during the 1970's resulted in broad laboratory use of EIS as a quantitative coating evaluation technique [2].

Today's use of EIS ranges from ranking candidate coating systems for corrosion protection performance to precise material property evaluations [3-13]. Researchers also conduct EIS investigations on coated structures [14-19]. Regardless of the application of EIS, it provides an important modern complement to the traditional, qualitative techniques that rely on visual analysis of coating defects.

2.1. Underlying Principals

The resistance, R , of a material governs its ability to prevent the flow of electric current. Ohm's law provides the relationship between the material's R and the experimental parameters of voltage, V , and current, I [11, 20]. The relationship applies only to DC signals. For AC signals, the signal is no longer constant, as with DC, but rather it becomes periodic and alternates, creating mathematically complex relationships. The derived material property for AC circuits is impedance, Z . Coating Z is dependent on angular frequency, ω , where $\omega = 2\pi f$ for frequency, f . See Equation 1 and Equation 2 for the DC and AC relationships, respectively.

$$R = \frac{V}{I} \quad \text{Equation 1}$$

$$Z(\omega) = \frac{V(\omega)}{I(\omega)} \quad \text{Equation 2}$$

The AC current response lags the sinusoidal voltage input, and the difference is the phase angle, θ . The exception is for a pure resistor, in which the voltage and current are in phase, i.e., $\theta = 0$ degrees and Ohm's law applies. Figure 1 provides a schematic of the current and voltage signals as a function of time, showing a phase angle of -90 degrees, or $-1/2\pi$, which is characteristic of a pure capacitor. Figure 1 uses a relative scale for voltage, $V(t)$, current, $I(t)$, and time, t .

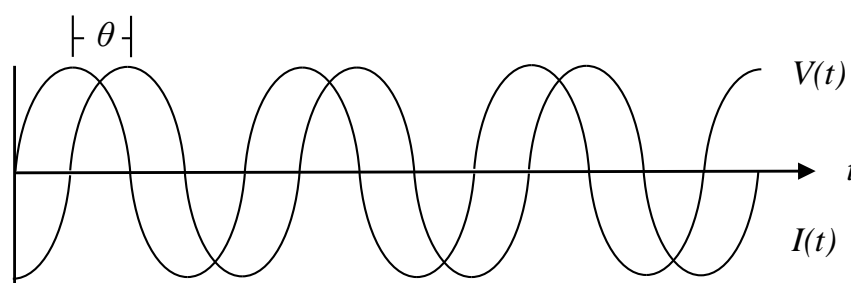


Figure 1. Schematic of sinusoidal applied voltage and current response as a function of time for EIS measurements.

Because EIS is an AC current technique, it provides a frequency-dependent analysis of material characteristics not provided by DC techniques, such as capacitance, C . Therefore, the primary benefit of EIS is that the resulting Z describes current flow through a coating to its substrate as a combination of both its R and C . These useful variables can be derived mathematically, or with software, to produce an equivalent circuit model (ECM) comprised of resistors and capacitors. Table 1 provides the relationships for these circuit elements. Note that the impedance relationship for C contains the imaginary number, $j = \sqrt{-1}$, in addition to ω .

Table 1. Impedance relationships for circuit resistances and capacitances.

Circuit Element	Ohm's Law Equivalent	Impedance Relationship
Resistor, Z_R	$Z_R = \frac{V_R}{I_R}$	$Z_R = R$
Capacitor, Z_C	$Z_C = \frac{V_C}{I_C}$	$Z_C = \frac{1}{j\omega C}$

The current flow through a coating follows one of two paths: 1) ionic charge transfer (a resistor), measured in ohms, or 2) stored charge (a capacitor), measured in farads (F). Therefore, the resistor-capacitor components for coating $Z(\omega)$ are in a parallel circuit, which can be described by the inverse relationship shown in Equation 3. By comparison, a series circuit would result in a direct relationship, $Z(\omega) = Z_R + Z_C$, but this circuit is not representative of current flow through a coating material unless corrosion is occurring at the substrate (see discussion below Figure 2).

$$\frac{1}{Z(\omega)} = \frac{1}{Z_R} + \frac{1}{Z_C} \tag{Equation 3}$$

Equation 3 is solved for $Z(\omega)$ in Equation 3, and Equation 4 substitutes the relationships in Table 1, deriving $Z(\omega)$ with respect to R and C .

$$Z(\omega) = \frac{1}{\frac{1}{Z_R} + \frac{1}{Z_C}} \tag{Equation 4}$$

$$Z(\omega) = \frac{1}{\frac{1}{R} + j\omega C} \tag{Equation 5}$$

Equation 5 allows for R and C to be considered individually while exploring the effect of ω on $Z(\omega)$. EIS resolves these resistive and capacitive characteristics of a material by applying a broad range of measurement frequencies. Figure 2 provides the resulting $|Z|(\omega)$ for three inputs of R and C , each within the range of values expected for an organic coating material.

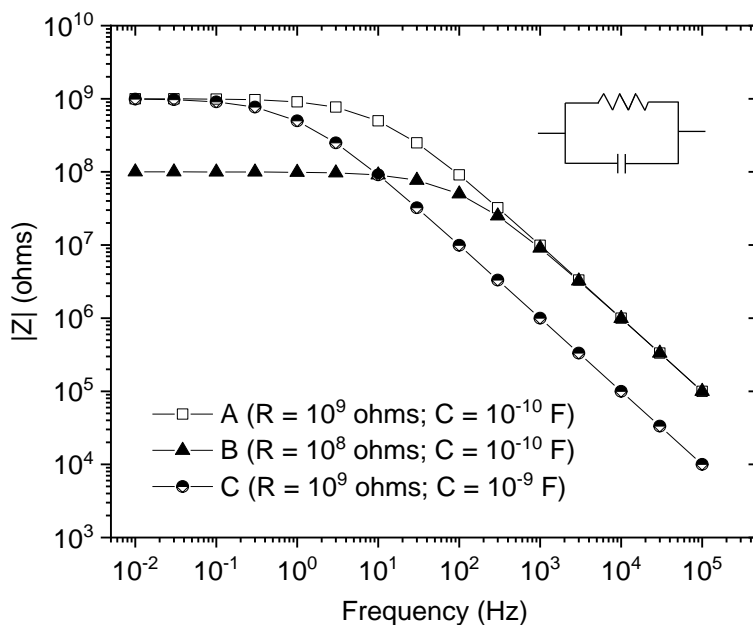


Figure 2. Parallel resistor-capacitor for three inputs of R and C .

Per Equation 5, the circuit capacitor is dependent on ω , as $j\omega C$. The frequency-dependent aspect of the capacitor is a function of the time requirement of charge storage; the more time allowed for current passage, the greater the charge that can be stored. Therefore, the parallel circuit results in insignificant current via the resistor when ω is very large and insignificant current via the capacitor when ω is very small. Put another way, current passes through the circuit capacitors as ω approaches infinity, ∞ , (high frequencies) and passes through the circuit resistors as ω approaches 0 (low frequencies).

Figure 2, above, illustrates the effect of measurement frequency on current flow. Examples A and B have equivalent capacitance, and their resulting impedance data is also equivalent at frequencies above 10^3 Hz. As the frequency decreases, the trend lines diverge, and the dissimilar resistance values become apparent (and equivalent to their element value) at frequencies below 10^0 Hz. Likewise, comparing Examples A and C reveals the dissimilar capacitance at high frequencies (a difference of one order of magnitude) and a convergence to their equal resistance, 10^9 ohms, at low frequencies.

A coating experiencing corrosion at the substrate requires a second parallel resistor-capacitor in series with the coating resistor. Here, current has the option to flow through the coating-steel interface via corrosion charge transfer (a resistor) or to become stored charge as part of the double layer (a capacitor). The circuit mathematics are more complex for this scenario but are easily handled by ECM software. Section 3.3. Deriving Material Properties further describes ECM analysis of EIS data.

2.2. Measurement Parameters

EIS has several parameters that must be user-defined. The median applied voltage and voltage amplitude are particularly important as they establish the sinusoidal voltage pattern that will be applied through the coating. The standard median applied voltage is open circuit potential (OCP) for the naturally corroding systems, determined by measurement at the onset of each test. An alternative approach is to set the voltage input value, based on the known or estimated OCP. The amplitude of the applied voltage is between 10 and 50 millivolts (mV) root mean squared. Very high impedance specimens may require the higher amplitudes.

The small voltage perturbation ensures the measurement is within the linear region of the polarization curve (applied potential, E , versus I , see Figure 3). Here, the slope equates to polarization resistance, R_p (Equation 6), which allows for calculation of corrosion rate, i_{corr} , via the Stern-Geary equation (Equation 7) [21]. The anodic and cathodic Tafel slopes, b_a and b_c , can be estimated.

$$R_p = \frac{\Delta E}{\Delta I} \quad \text{Equation 6}$$

$$i_{corr} = \frac{1}{R_p} \times \frac{b_a \times b_c}{2.3(b_a + b_c)} \quad \text{Equation 7}$$

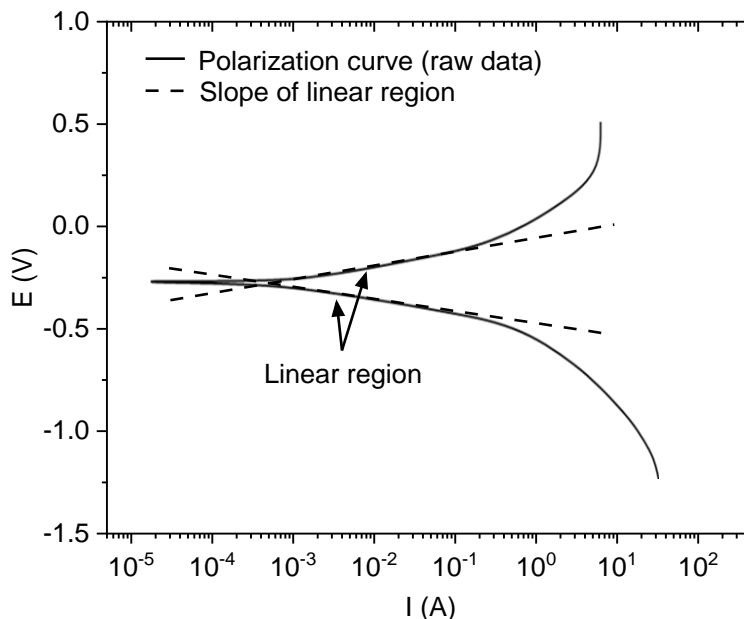


Figure 3. Schematic polarization curve with approximate EIS analysis location (linear region) identified.

The frequency range of an EIS measurement must also be defined. EIS generally employs many frequencies; a typical range for coatings is 10^5 to 10^{-2} Hz, which is sufficient to expose the resistive and capacitive properties of the material. The actual number of frequencies measured within that range is often described as “points per decade.” Selecting ten points per decade provides a very thorough analysis. However, this number can be reduced significantly, which also has the effect of shortening the test time. Applying five points per decade allows for a much shorter test period with minimal detriment to the data.

See the test method sections for measurement parameter recommendations and software images.

2.3. Raw Data Presentation and Interpretation

The evaluation of materials with EIS provides a complex dataset. Polar (complex plane) and Cartesian coordinate presentations of this data are common, and each reveal useful information. Plotting the data via polar coordinates is known as the Nyquist plot, shown in Figure 4(a). The Nyquist plot displays real and imaginary Z values, as Z_{real} and Z_{imag} , respectively. A negative scale is shown for Z_{imag} because the current data lags the voltage, i.e., $\theta < 0$. The plot must show both axes at the same scale so that the plot is square, which allows for proportionate viewing of the results. The radius of each data point in the Nyquist plot is the Z magnitude, $|Z|$, and the angle to the x-axis is the θ ; derivation of these two values provides the Bode plot in Figure 4(b). Put another way, the Nyquist plot has coordinates (Z_{real}, Z_{imag}) , and the Bode plot presents the $(|Z|, \theta)$ coordinates individually versus the measurement frequency.

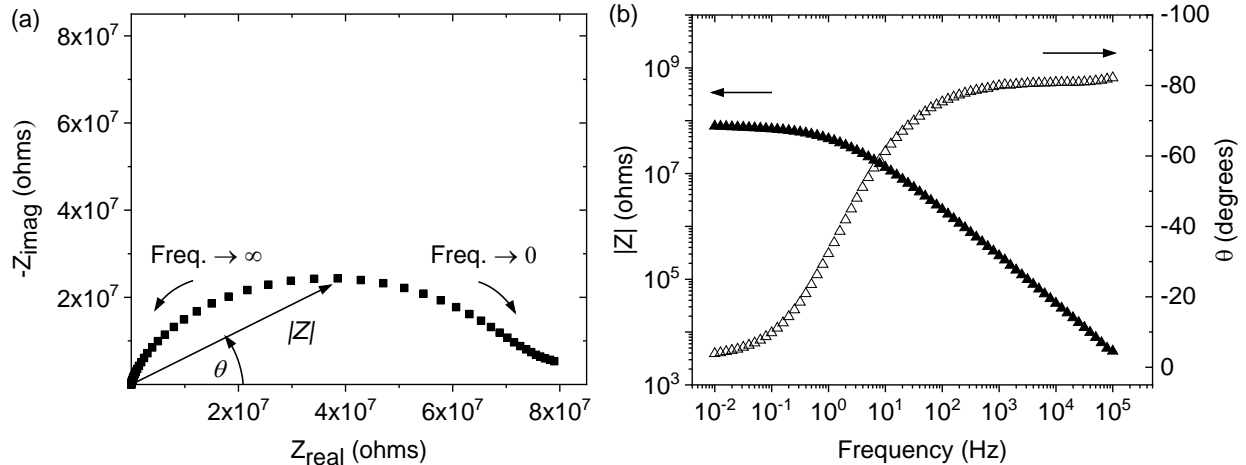


Figure 4. EIS data presented by (a) Nyquist plot and (b) Bode plot.

An advantage of the Nyquist plot is that the number of resistor-capacitor components needed to describe the data, known as the number of time constants, is often apparent as unique semi-circles in the curve. The Figure 4 data demonstrates one time constant. As a further example, two time constants would indicate the use of two resistor-capacitors pairs to describe the data, which is generally the case for a coating experiencing corrosion at the substrate (see Figure 5(a) for example). The Nyquist plot also allows for discernment of pure resistance values directly from the plot. Recall that resistors in an AC circuit do not have a current lag, so there is no imaginary contribution to impedance. Therefore, $R = Z_{real}$ when $Z_{imag} = 0$.

A disadvantage of the Nyquist plot is that the measurement frequency values are indiscernible. The frequency approaches ∞ as the data nears the origin, and it approaches 0 in the opposite direction. Furthermore, the axis scales are linear, and low resistance values cannot be distinguished near the origin.

EIS data presentation by the Bode plot shows $|Z|$ and θ versus measurement frequency and converts all scales to logarithmic. Figure 4(b) provides an example Bode plot that combines the two dependent variables onto one plot (the left y-axis for $|Z|$ and the right y-axis for θ); it can also be shown as two separate plots.

An advantage of the Bode plot is that the measurement frequency is apparent for all data. Comparing the measurement frequency with the measured θ reveals the circuit behavior in terms of known circuit elements, such as a resistor ($\theta = 0$ degrees) or a capacitor ($\theta = -90$ degrees). Figure 4(b) shows circuit behavior representative of a capacitor at frequencies above 10³ Hz and of a resistor at frequencies below 10⁰ Hz. The behavior is analogous to Figure 2, above, which revealed the effect of current flow through the resistor-capacitor elements as $|Z|(\omega)$. The $|Z|$ curve in Figure 4(b) is comparable to Figure 2 and, from which, may be approximated (by the trained eye) to have properties of $R = 10^8$ ohms and $C = 10^{-9}$ F.

A disadvantage of the Bode plot is that it requires plotting two sets of information rather than one. Further, the logarithmic scales make interpreting raw values an approximation by order of magnitude.

Interpretation of both the Nyquist and Bode plots reveal nuances via the shape of the curve. Figure 4(a) shows a depressed semi-circle on the Nyquist plot, which indicates that the coating material is not a perfect capacitor, as is usually the case. Figure 5(a) provides schematics of other possible features on a Nyquist plot, which includes a Warburg element, marked by a 45-degree tail at the low frequencies (slope of 1), which is the result of diffusion-controlled reactions [11]. Figure 5(a) also shows an example of inductance, shown by a loop into the positive Z_{imag} quadrant at the low frequencies as well as a curve containing two time constants. The two time constants curve presents an ideal scenario; in practice the two semi-circles often overlap and require computer modeling to resolve the individual resistor values. Per the given schematic the first resistor-capacitor would intercept the x-axis around 1.5×10^7 ohms and, subsequently, represent the value of the resistor. Similarly, the second resistor-capacitor would intercept around 6.0×10^7 ohms and have an approximated value of 4.5×10^7 ohms, i.e., $6.0 \times 10^7 - 1.5 \times 10^7$ ohms.

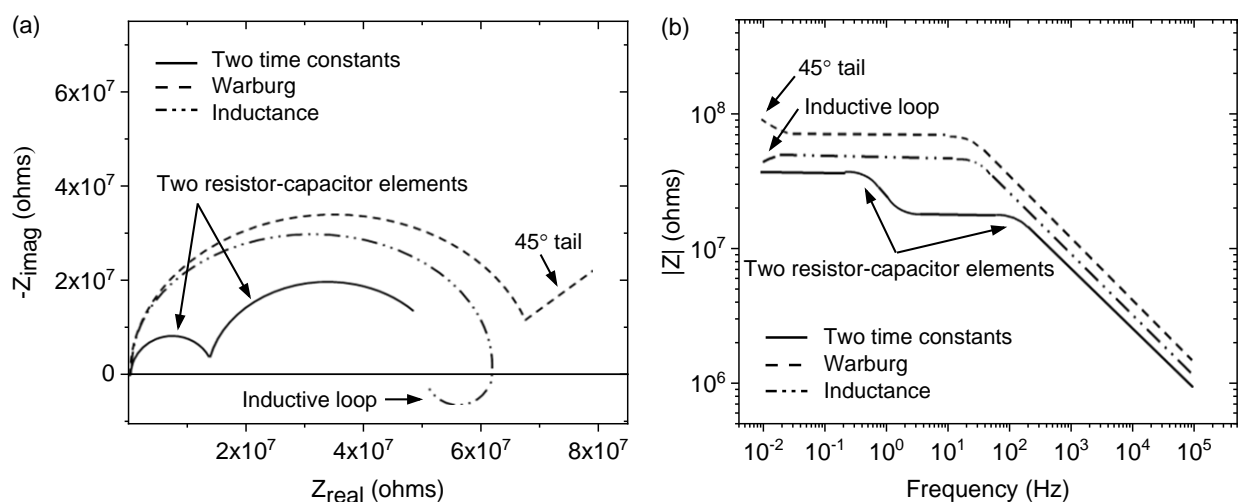


Figure 5. Schematic curves for two time constants, Warburg diffusion, and inductance as (a) Nyquist and (b) Bode plots (impedance magnitude only).

Figure 5(b) provides the schematics for two time constants, Warburg element, and inductance on a Bode Plot. Notice that the characteristic shape for the two time constants schematic is apparent. In practice, one of the resistors often has a much lower value and can only be observed by zooming in at the origin or by viewing the Bode plot. The Warburg element and inductance examples are subtler in Figure 5(b).

A significant body of literature is available to extract information from these curves, including breakpoint frequency [22], in which the circuit changes between resistive-capacitive behavior, coating adhesion [23], exposed substrate area (pores) [24], and others [6, 25-27]. Still more

sophisticated analyses consider the inhomogeneity of coatings, and the predominance of EIS current flow to substrate cathodes as opposed to anodes [28, 29].

3. Analysis of EIS Data Sets

The types of data collected ranges from laboratory evaluation of newly applied coating material to field evaluation of coatings after many decades of in-service exposure. The sections below provide analysis procedures that are relevant to either scenario but may find greater use in certain applications.

3.1. Coating Sampling (Estimating Coating Quality)

Estimating coating quality often requires testing of multiple samples. This is true not only of EIS testing, but also of other techniques (e.g., dry film thickness testing). A statistically sound sampling approach ensures that the evaluation of a large area of coating provides useful data.

Laboratory EIS analysis may use small sample sizes, generally one to five specimens of coated coupons (approximately one square foot (ft²) or less). The low sample number may still prove useful because of the good experimental controls that are possible in the lab. Therefore, laboratory EIS is a screening method for coating quality, and the few specimens evaluated, often of freshly applied coating systems, is generally sufficient to suggest the anticipated barrier performance of that system.

Field EIS analysis evaluates coated structures, the total surface area of which may be in the range of 10³ to 10⁶ ft². Furthermore, the value of field EIS analysis is that it supplements traditional coating assessments with quantitative information for decision-making purposes. The decisions may have high cost implications, so it is imperative to use robust statistical analysis of a reliable data set. A trained investigator ensures that each data set is reliable. The EIS testing must produce an appropriate sample size for statistical analysis that considers variability in coating application quality, degradation, etc. Mathematical theory often suggests a sample size of 30; therefore, this is the recommended sample size for EIS field testing. The size of the structure, cost associated with the maintenance decision, inaccessibility, or other risk factors should be drivers for determining the degree of compliance with this recommendation. As an example, there is a strong recommendation to meet or exceed a sample size of 30 for large structures (nearing 10⁵ ft²); these structures are not easily accessible and typically cost more than \$1 million to perform coating maintenance.

EIS field testing should use either a random or regular sampling approach. An example of a regular approach is to test at regular intervals along a pipeline. In planning for the inspection, determine the pipe length (or the total number of pipe sections) and calculate a sampling rate that produces at least 30 EIS data sets. Larger data sets may be appropriate if time allows. Sampling rate along a pipeline should also be sufficient to resolve differences in the coating quality along the pipe alignment. Smaller data sets (10 to 20 specimens) may be appropriate for smaller structures, such as gates, and should, again, scale in accordance with the previously specified drivers. Random sampling should include documentation of each specimen location to aid in the data analysis and identify possible causes for anomalies.

3.1.1. Low Frequency Impedance

The low frequency impedance, usually 10^0 Hz or lower, is an important analytical feature of EIS testing. Here, the data represents the coating resistance, as discussed in Section 2.1. Underlying Principals. EIS data of aged coatings on structures often contain additional resistances associated with substrate corrosion. These additional resistances are additive, and the low frequency impedance value includes all resistances in the circuit. Therefore, the low frequency impedance indicates the overall corrosion protection provided to the substrate. The EIS data indicates excellent corrosion protection at values greater than 10^8 ohms at 0.1 Hz, and insufficient protection below 10^6 ohms [1, 30]. These values apply to both lab and field EIS testing and have their respective implications [31]. Lab evaluations of coatings systems should sustain values greater than 10^8 ohms, but preferably 10^9 ohms, for several years of weathering exposure to be candidates for specification on structures. Coatings on structures can remain in service provided they continue to meet the 10^8 ohms threshold.

Figure 6 provides an example of field EIS data for a large pipeline interior coating, shown as the low frequency impedance magnitude at 0.05 Hz, $|Z|_{0.05 \text{ Hz}}$, (total coating resistance) versus the location in the pipe. The pipeline structure serves as a siphon with several steep slopes, and, therefore a corresponding elevation plot is inset for reference to possible hydraulic service conditions, which may contribute to accelerated coating degradation. The results indicate several data points less than 10^8 ohms, particularly near the inlet, outlet, and steep slopes adjacent to the lowest elevations of the siphon. The data suggests that corrosion protection is not adequate at the lowered-numbered pipe segments, approximately, 0 to 100, due to the presence of many $|Z|_{0.05 \text{ Hz}}$ data points below 10^8 ohms. Note that data is absent between pipe segments 40 to 60 because access to this area was not possible during the inspection. In contrast, the second half of the pipe, approximately pipe segment 120 to 190, is receiving excellent corrosion protection.

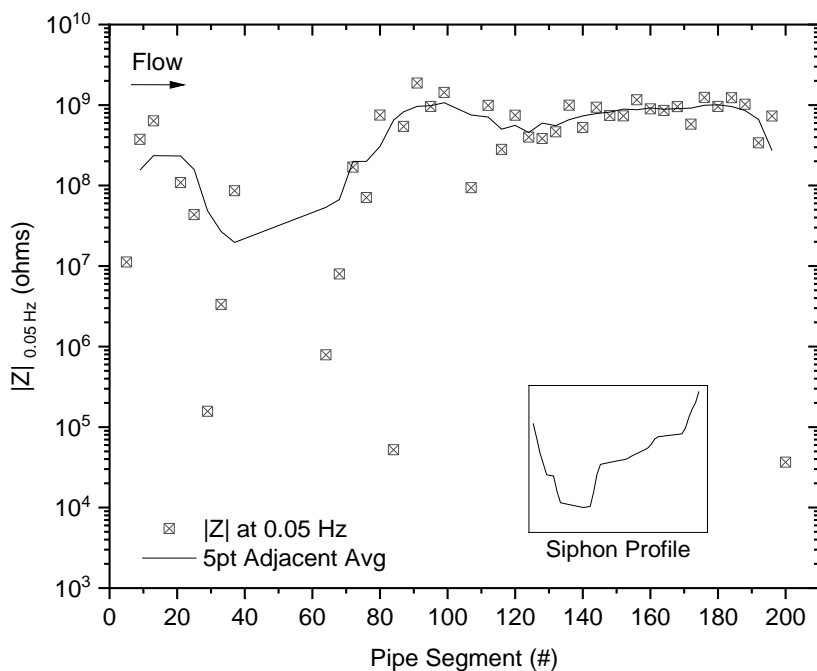


Figure 6. Impedance magnitude at 0.05 Hz versus pipe segment; corresponding elevations inset.

The results within Figure 6 demonstrate that a large dataset is critical to accurately portray the coating quality on an existing structure. In this case the data suggests that coating quality is not consistent throughout the structure, and pipe segments in the first half of the pipe are priority locations for coating maintenance. Data from traditional field assessment techniques, including visual inspection, should accompany the EIS data when determining final recommendations for maintenance.

3.1.2. Probability Plot

A lognormal probability plot of the low frequency impedance data provides a pass/fail approach for evaluating coating quality [31, 32]. The method is consistent with an existing approach for the evaluation of soil resistivity [33]. It designates the allowable risk for coating quality via statistics and assumes uniform coating degradation. Figure 7 provides an example of field EIS data from three coatings. The x-axis is the calculated percentiles, identifying the probability that the mean $|Z|_{0.05 \text{ Hz}}$ for the corrosion protection is less than this x-axis value. The plot contains a dotted line at 10% probability and linear trendlines for each data set. Origin software (OriginLab Corporation ©, Northampton, MA) provides a probability plot option, allowing for easy plot development as well as the addition of the linear trendlines.

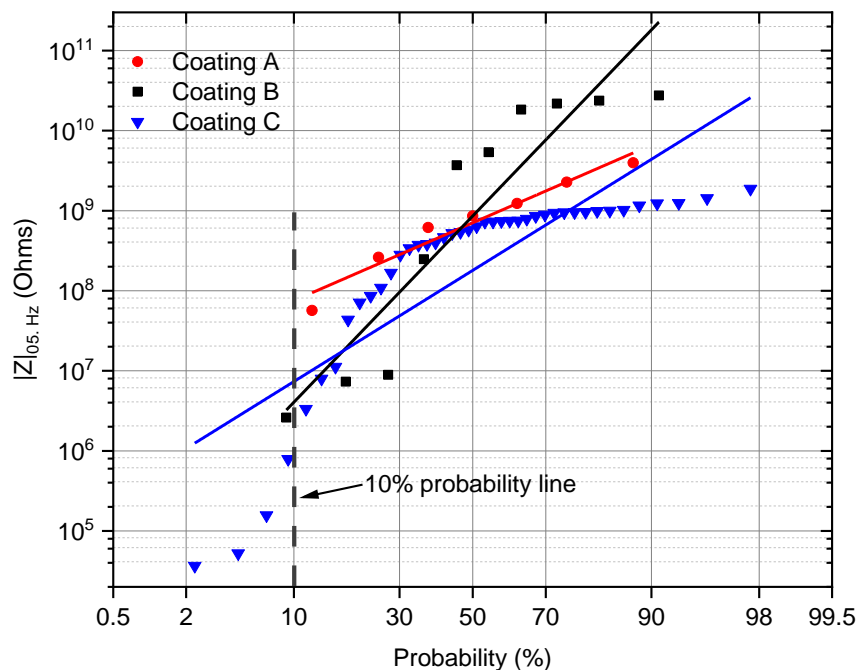


Figure 7. Probability plot of low frequency impedance data (reproduced from [31]).

The 10% probability plot establishes pass/fail criteria for the $|Z|_{0.05 \text{ Hz}}$ trendline at 10% probability. The coating quality passes if the impedance trendline is greater than the prescribed value at 10% probability and fails if it is lower. Using Figure 7 as the example, a $|Z|_{0.05 \text{ Hz}}$ criterion of 10^7 ohms results in a “pass” for Coating A and a “fail” for Coating B and Coating C.

Figure 7 allows for several additional conclusions to be drawn. First, the $|Z|_{0.05 \text{ Hz}}$ data should be linear on the plot. Non-linear data does not follow a lognormal distribution, which is a

prerequisite for probability plot analysis and is an indication of bias or other factors contributing to the results. Coating C is perhaps the obvious example of non-linear data in Figure 7, as most of the data is a large distance from the linear trendline. Coating C is the Figure 6 data, and the changing hydraulic conditions along the pipe, i.e., non-uniform degradation, are likely contributing to the non-linear result. Interpreting non-linear 10% probability results for decision-making purposes is inconclusive; instead, a non-statistical EIS analysis should occur, such as in Section 3.1.1. Low Frequency Impedance, while incorporating other available data.

The Figure 7 results also demonstrate the effect of insufficient data (see Coating A and Coating B). In both cases, the linear trendline fails to surpass the 10% probability line by a large amount, or at all for Coating A. Therefore, the confidence of these trendlines is also inadequate for decision-making purposes.

3.2. Longitudinal Analysis (Estimating Service Life)

Plotting EIS data at progressive exposure times allows for the evaluation of coating degradation or other coating quality changes. Applying trendlines to the resulting data set provides a hypothetical extrapolation for past or future coating quality. This approach is a longitudinal analysis, which provides an estimation of the coating service life. The technique is applicable to lab or field analyses.

Lab analysis often evaluates a coating during the initial weeks or months of its exposure. Figure 8 provides an example of $|Z|_{0.01\text{ Hz}}$ versus exposure time for a laboratory coupon. The data includes testing during exposure for as many as 10 years and includes a fitted line to approximate the trajectory of changes to the coating properties via first (linear), second, or third degree polynomial functions. The data for the first year is abundant, and it captures changes that occur when water enters a coating, which is a period of degradation. Coating B and D show a significant reduction in $|Z|_{0.01\text{ Hz}}$ during the first year of exposure. The polymer matrix adjustments within Coating A, B, and D demonstrate a steady-state after several months of exposure in Figure 8, and $|Z|_{0.01\text{ Hz}}$ becomes relatively constant for 5 or more years. Coating B is relatively unchanged during the entire exposure period, shown by a linear trendline, whereas Coating A reveals a sharp decline after 8 years. Coating E shows a linear degradation over the duration of the exposure time, and Coating C is approximately second degree polynomial degradation. Each coating includes an abundance of data at the end of the exposure (weekly testing) to enhance the dataset. The examples in Figure 8 illustrate a variety of degradation patterns that are possible for coating systems. The long-term testing is valuable to identify subsequent degradation events that indicate coating failure, such as occurs for Coating A after 8 years of exposure.

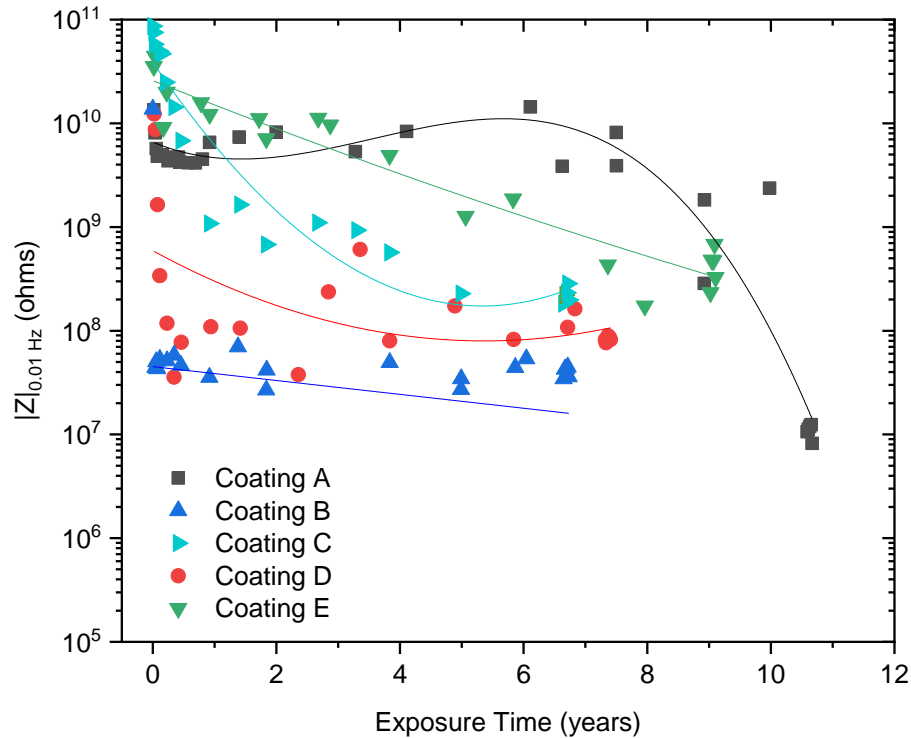


Figure 8. Low frequency EIS data versus time of exposure.

Regular access to field structures is typically not feasible, which precludes the longitudinal analysis of field EIS data. Incorporating field EIS testing into regular coating assessments could result in future longitudinal analysis opportunities for structures, which would improve estimations of the coating quality and remaining service life.

Longitudinal data analysis to estimate coating service life has tremendous potential future benefit for coating maintenance as well as the coating industry. Multiple research groups attempted to mathematically describe the degradation of coating impedance properties to estimate service life [34-37]. The previous efforts utilized laboratory analysis, which allows for good control of experimental variables, but a verifiable approach for estimating service life is not yet available. Future efforts should include regular EIS testing on coated structures and address the enormous complexity of variables that govern coating performance, such as the environment conditions during coating application and in service.

3.3. Deriving Material Properties

Advanced analyses for EIS data sets include ECM and deriving material properties. ECM is a common approach that results in describing the material by physical circuit elements. This can help to determine the processes occurring through the coating material and at the substrate interface. The physical circuit elements also allow for calculations of the material resistivity and the dielectric constant. The previously presented analyses, i.e., statistical analysis of a large sample set or evaluation of the change in the property after exposure, are all options for treatment of any derived values.

3.3.1. Equivalent Circuit Modeling of Coatings

ECM describes the impedance data as a combination of circuit elements [4, 11, 38-40]. The modern ECM approach employs software to perform the analysis, which applies resistor-capacitor elements in defined arrangements. Equation 5 is the basis of the simplest circuit used in the evaluation of coating materials. This circuit, called the Simplified Randles cell [41], includes an additional resistor, R_s , to account for the electrolyte solution resistance, which should be insignificant. For the coating R and C in this circuit, R_{pore} = pore resistance and C_c = coating capacitance. The R_{pore} is the ionic charge transfer through the aqueous or semi-aqueous pores and channels within the coating bulk. The C_c is the ability of the coating bulk to store charge.

The ECM software output is the value(s) of its circuit elements. As an example, Figure 2, above, provided the opposite approach. The model began with the circuit element values (listed within the figure) and resulted in the illustrated curve. The ECM software applies an iterative process to solve the circuit element values for the given curve (EIS data) based on the user-defined circuit elements. In addition to the raw data, the ECM software requires two additional inputs 1) an appropriate and realistic ECM and 2) approximated ECM element values. The software uses the approximated values in its first iteration of the ECM and implements a fitting analysis of subsequent iterations to produce a solution.

Figure 9 provides the ECM fitting results for a coating material using a Simplified Randles cell. The raw data points are shown and include a solid red line; the fit result is a solid green line. The example includes both the Nyquist and Bode plot to evaluate the fit result by linear and logarithmic scales. For this case, the Nyquist plot does not show strong congruence between the raw data and fit results. Likewise, the Bode plot also shows a poor fit, particularly for θ , i.e. “theta.” The raw data on the $|Z|$ plot between 10^1 and 10^4 Hz has a shallower slope than the fit result, which is indicative of the coating material not behaving as a pure capacitor. Additional checks of this conclusion are apparent on the theta plot, where $\theta = -70$ degrees rather than -90 degrees (pure capacitor), and, similarly, the Nyquist plot reveals a depressed semi-circle.

To resolve the imperfect capacitance of coating materials, a constant phase element (CPE), CPE_{coat} , replaces the C_c element [42]. The CPE is a circuit element with characteristics ranging from resistor to capacitor, which greatly enhances the flexibility of the ECM process. The CPE exponent, α , with values between 1 and -1 , accounts for the phase shift of the AC current response, i.e., θ , in accordance with Equation 8.

$$\theta = \frac{\pi}{2} \times \alpha \quad \text{Equation 8}$$

Therefore, for a pure resistor, $\alpha = 0$ and for a pure capacitor, $\alpha = -1$. Figure 10 provides the revised ECM fit results, showing excellent agreement with the raw data on both the Nyquist and Bode plots. Notice that $\alpha = 0.77$ (shown as CPE_{coat-P} within the Nyquist plot), which is typical of a coating material.

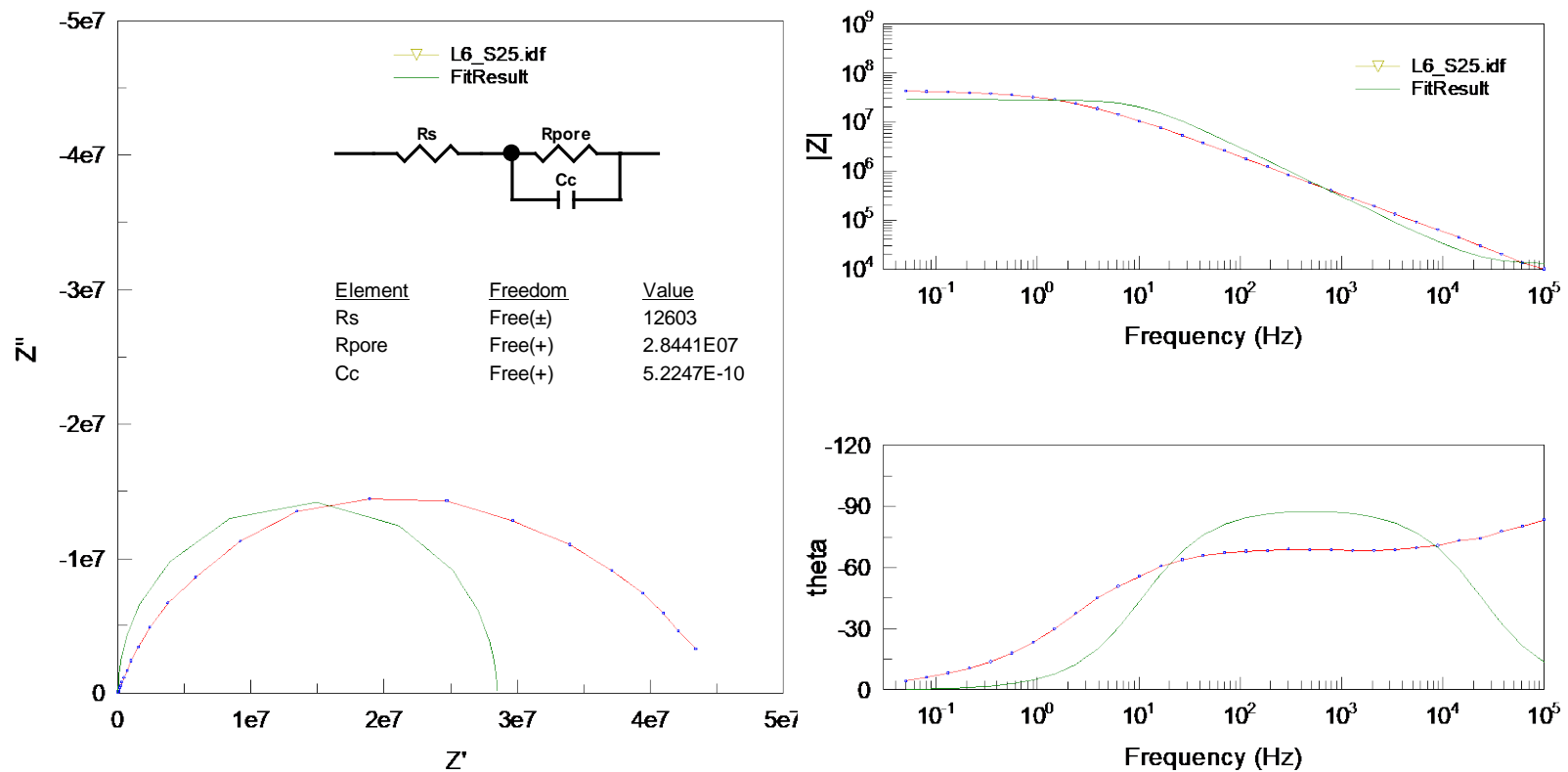


Figure 9. ECM fitting results for a simple Randles cell by (left) Nyquist and (right) Bode plots.

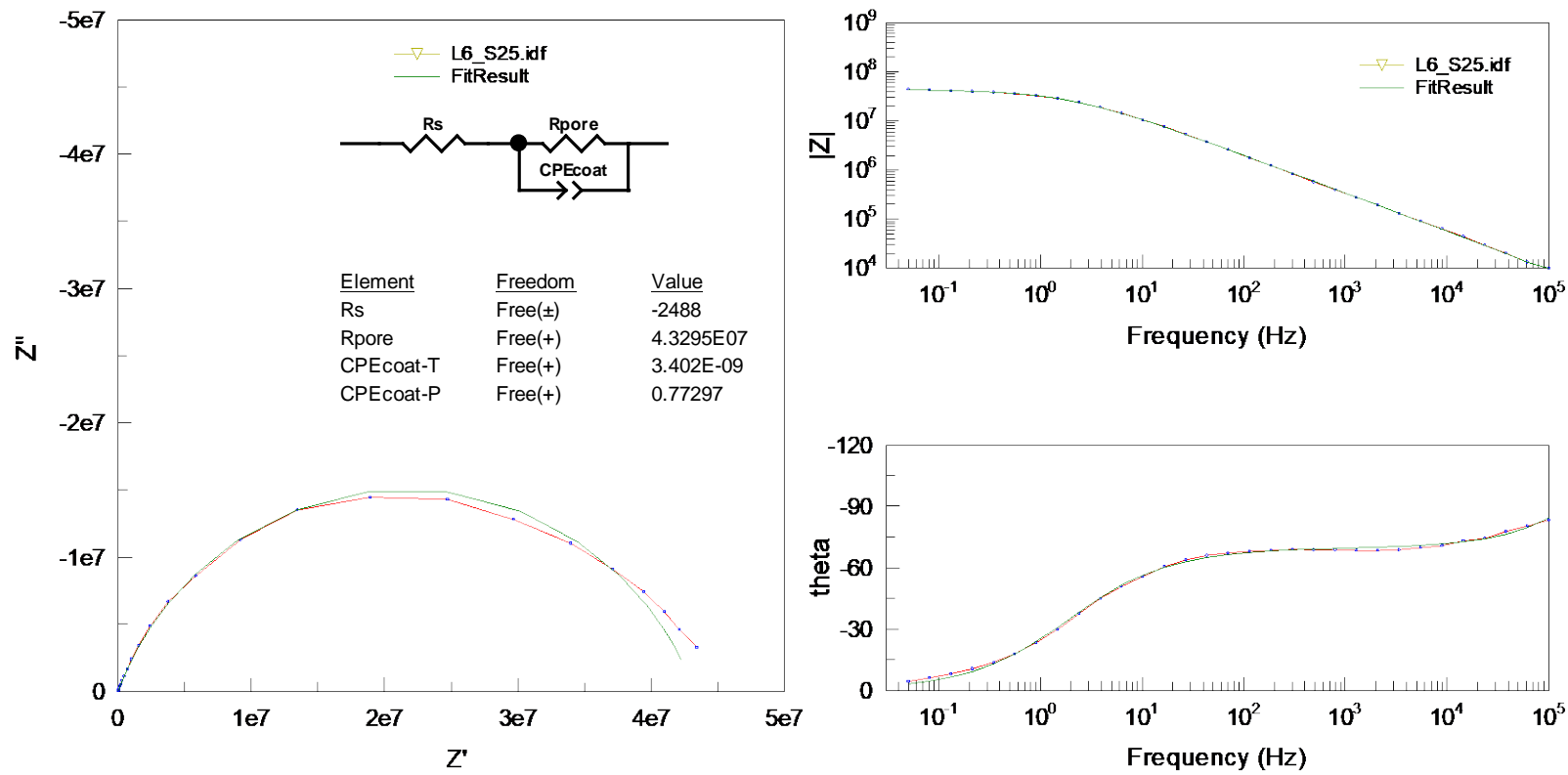


Figure 10. ECM fitting results resistor-capacitor revised with constant phase element by (left) Nyquist and (right) Bode plots.

Electrochemical evaluations of bare metal substrates also employ the Simplified Randles cell, where R_{ct} = charge transfer resistance and C_{dl} = double layer capacitance. The R_{ct} is the ionic charge transfer across the interface, i.e., corrosion reactions. The C_{dl} is the phenomenon in which stored charge organizes across an interface. However, a coating experiencing corrosion at the substrate requires two resistor-capacitor pairs. The resistor-capacitor pair for corrosion at the substrate is in series with R_{pore} , as shown in Figure 11. Physically, this equates to current flow through the coating via ionic charge transfer, resulting in either 1) charge transfer across the interface (corrosion), or 2) stored charge at the interface.

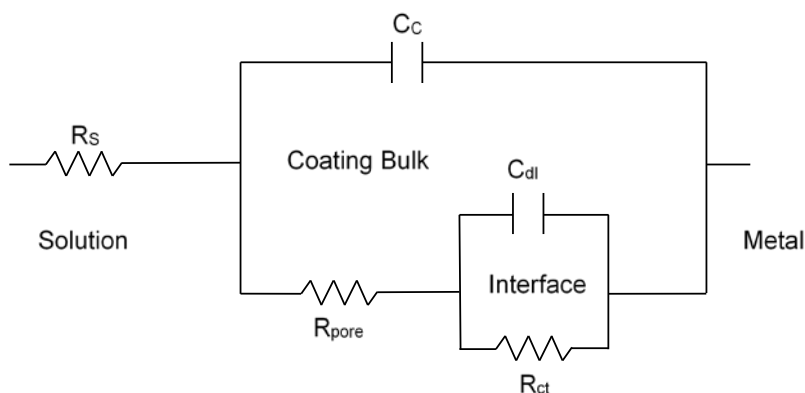


Figure 11. Coating equivalent circuit model with traditional circuit elements

The EIS data for a good barrier coating is unlikely to reveal a significant contribution for the resistor-capacitor pair at the interface. A good barrier coating, by definition, acts as a capacitor (stores charge). As ionic pathways develop through the coating bulk, the current flow through these pathways eventually becomes significant. The EIS data reflects this by the introduction of resistive behavior at the low frequencies. Upon further coating degradation and establishment of corrosion reactions at the interface, the second resistor-capacitor pair becomes significant in the EIS data. The revelation of two time-constants is most apparent when the R_{pore} and R_{ct} approximate each other in magnitude. See the two time constants schematic within Figure 5 of 2.3. Raw Data Presentation and Interpretation as an example EIS data set that has two comparable resistors.

3.3.2. Physical Material Properties

EIS data, and corresponding ECM results, also allows for derivation of coating material resistivity and dielectric constant. The resistivity, ρ , is a simple function of the coating R and its geometry, the area, A , and distance, d (Equation 9). The resistivity has units of ohm-cm and is the reciprocal of the conductivity, i.e., the ease with which the material transmits current.

$$R = \rho \frac{d}{A} \quad \text{Equation 9}$$

The dielectric constant, ϵ , is a unitless, relative term that describes the electrical permittivity of a material (Equation 10). The permittivity of a vacuum, ϵ_0 , (8.85×10^{-14} F/cm and $\epsilon = 1$) provides the basis for this property, which is also a function of the geometry of the material.

$$C = \frac{\epsilon_0 \epsilon A}{d} \quad \text{Equation 10}$$

The changes to these variables over the course of coating exposure can be used describe physical phenomena or material degradations. For example, ϵ changes as a function of the volume percent of water in the coating because of the large relative difference between the permittivity of water (80) and polymer (approximately 2 to 8) [11, 25].

4. EIS Measurement Procedures

Modern instruments perform the potentiostatic EIS experiments using dedicated software. EIS testing uses four lead wires for the measurements. Two lead wires measure current through a high impedance resistor circuit and two measure and control voltage through a separate circuit. The current flows between the working electrode (WE) and counter electrode (CE) and is the dependent variable in the experiment. Voltage regulation occurs between the reference electrode (RE) and a second voltage lead wire within the WE.

4.1. Laboratory EIS Testing

A galvanostat/potentiostat, such as the FAS2 Femtostat from Gamry Instruments (Warminster, PA) or equivalent, is a suitable instrument for laboratory EIS testing. The test set up uses the following three electrodes:

- WE – The metallic (conductive) substrate of a coated coupon, such as 3-inch x 6-inch x 0.375-inch steel panels prepared and coated according to the manufacturer's product data sheets. A corner or edge must be ground or filed to bare steel to provide a low resistance electrical connection for the electrode. Evaluation of free films requires a conductive medium on both sides of the film, typically by using commercial glassware designed for such use.
- CE – A platinum (Pt) mesh or other conductive and inert material with a large surface area and high exchange current density.
- RE – Laboratory grade saturated calomel electrode (SCE), silver-silver chloride electrode (SSCE), or copper-copper sulfate electrode (CSE). If necessary, a conductive, inert material is suitable.

4.1.1. Materials

Table 2 provides a list of laboratory EIS equipment items. The glass cylinder, *o*-ring, clamp, and dielectric material make up the physical test cell, but alternative test cell materials are possible. Laboratory EIS testing requires a continuous and electrically grounded Faraday cage helps to reduce external electrochemical noise in the data. Faraday cage designs range from wood frames covered with copper mesh or foil material to commercial cabinets. Electrolyte for the test cell provides a known, low resistance medium to transmit current between the electrodes and the coating surface. Possible electrolyte solutions include 5 weight percent (wt. %) sodium chloride (NaCl) and dilute Harrison's solution (DHS—0.35 wt. % ammonium sulfate ((NH₄)₂SO₄) and 0.05 wt. % NaCl).

Table 2. Equipment items for laboratory EIS testing

• Potentiostat	• Glass cylinder	• Saturated calomel electrode (RE)
• Computer/processor	• O-ring	• Platinum mesh (CE)
• Faraday cage	• Clamp	• Coated metal coupon (WE)
• Electrolyte	• Dielectric material	

4.1.2. Method

Below is a step-by-step method for performing EIS testing on coated metal coupons. It includes footnotes to further describe pertinent items or provide the user with additional information.

1. Determine the test schedule for the experiment, which designates the exposure period between each measurement. A freshly applied coating system should receive weekly testing during the initial months to observe changes associated with water ingress. Afterward, the testing interval may lengthen through the end of the first year of exposure. Long-term test evaluations vary from annual to more frequent test intervals. An example schedule proposes testing in accordance the following accumulated weeks of exposure: 1, 2, 3, 4, 6, 12, 18, 24, 48, 72, 96, etc.
2. Expose coated coupons to simulate or accelerate weathering in the laboratory. Common techniques include ASTM B117 salt fog, ASTM D5894 cohesion, ASTM D870, and immersion in DHS (modified ASTM D870).
3. Remove coated coupon from exposure environment and gently wipe dry. Place dielectric material beneath the coated sample and clamp glass cylinder to the coating surface using an *o*-ring. Add dilute salt solution that is equivalent to the test exposure, such as DHS.
4. Place a SCE and Pt mesh within test cell and set within the Faraday cage. Connect to RE and CE instrument lead wires, respectively.¹ Connect WE instrument lead to coated coupon substrate, ensuring good metal-metal contact by filing or grinding iron oxides as needed. Figure 12 provides a completed set-up within a Faraday cage.

¹ Follow manufacturer's guidelines for reference electrode use and care. Check potential using a voltmeter regularly. Replace saline solution when potential drifts ± 5 mV from a calibrated electrode. Adjust rubber sleeve to open atmosphere while testing and keep closed in storage.

5. Boot computer and open the potentiostat software. Select “Potentiostatic EIS” test option or equivalent. Adjust test parameters to meet testing requirements (Figure 13), e.g., see Table 3 for recommended parameters, which are adequate for most measurements. Consult the equipment manufacturer’s customer service representative for additional support.²
6. Begin experiment. Monitor the open circuit potential (OCP) measurement to ensure the system is at steady state, i.e. the OCP is not increasing or decreasing systematically. An acceptable allowance for potential drift is ± 50 mV per 100 sec, assuming the raw value is between +500 and –1500 mV vs SCE. Stop the experiment for OCP exceeding ± 3000 mV vs SCE and assess the instrument lead wire connections.³
7. Measurement duration is dependent on measurement parameters, and thirty minutes is typical for the Table 3 parameters. Ensure the test finishes, the data set is reasonable (see Figure 14), and the data file saves to the intended location. Repeat the test if uncertain, allow one day for coating to equilibrate again if repeat test also appears errant.
8. Disassemble test cell and return coated coupon to laboratory weathering exposure.

² Parameters such as Stabilization, Cycles, Repeats, and Gains are variables that balance time-of-experiment with quality of data (noise reduction). Increase the End Frequency to shorten the test time and reduce the End Frequency to increase the quantity of low frequency data.

³ Immersing in DHS exposure and testing with DHS solution should keep the coated coupon at steady state. If not, keep the test cell and solution undisturbed for 30 minutes prior to testing. Very high barrier coatings and first-time exposure coatings may have too high of an impedance for accurate testing because it exceeds the instrument’s limit.

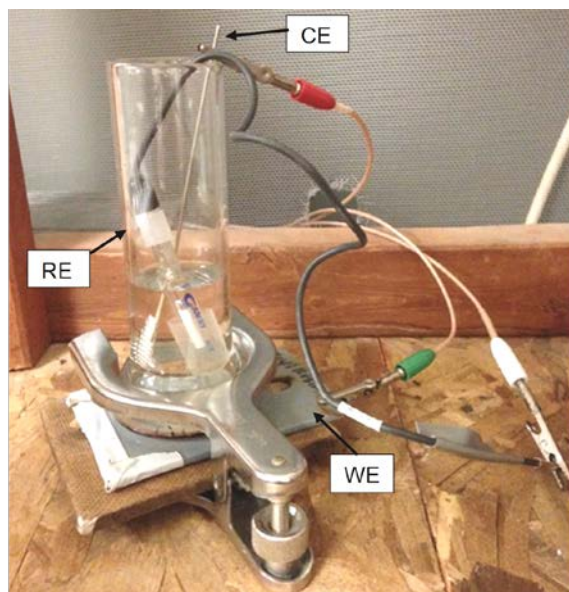


Figure 12. Test cell set-up within Faraday cage for EIS.

Table 3. Recommended EIS parameters and inputs

Parameter	Input
Open Circuit Potential (OCP)	100 seconds (sec)
Start Frequency	10^5 Hz
End Frequency	10^{-2} Hz
Voltage Amplitude	10 mV
Points per Decade	10

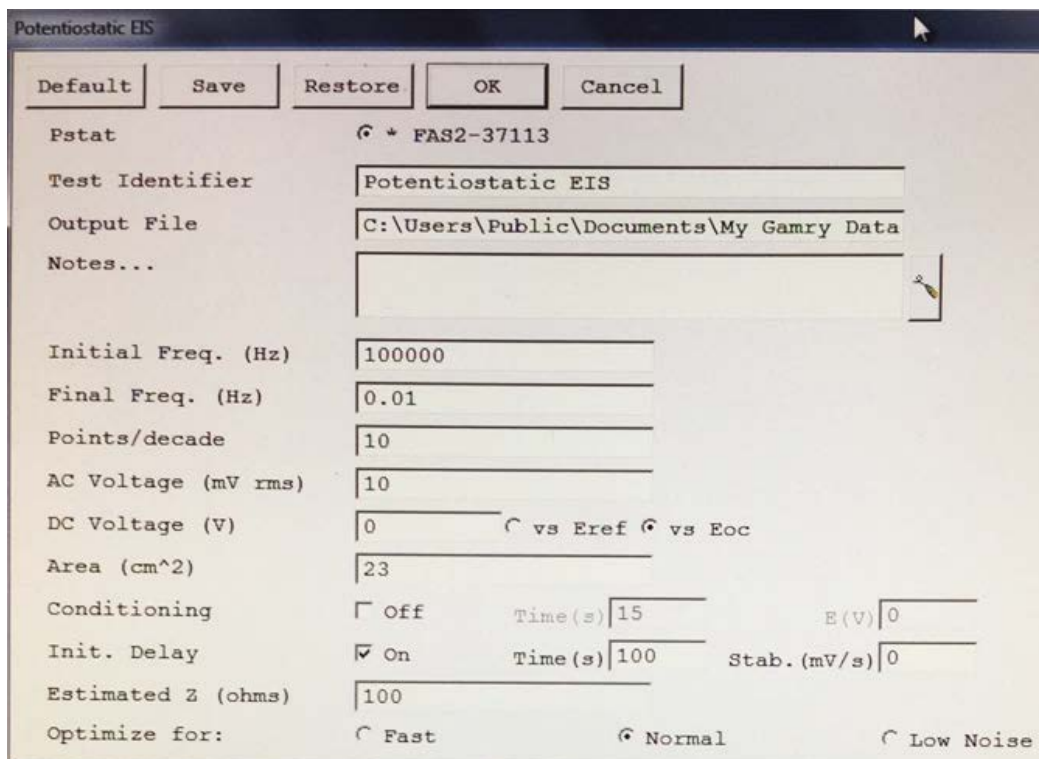


Figure 13. Screenshot of potentiostatic EIS typical test parameters and inputs.

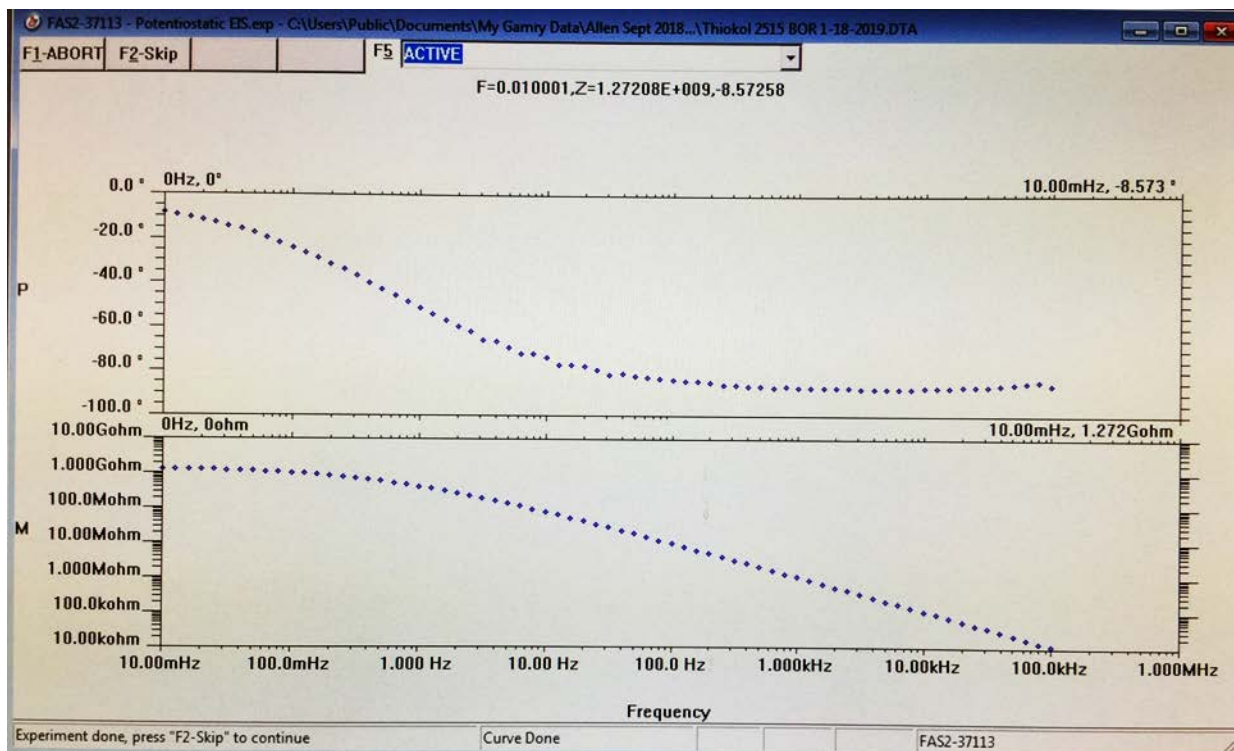


Figure 14. Screenshot of completed EIS test Bode plot showing phase angle (top) and impedance magnitude (bottom).

4.2. Field EIS Coating Inspection

A mobile or portable galvanostat/potentiostat, such as the CompactStat.e10800 from Ivium Technologies B.V. (Eindhoven, The Netherlands) or equivalent, is a suitable instrument for field coating inspections. The instrument must utilize a DC power source, such as batteries or a USB laptop connection. The field EIS test method requires no connection to the substrate and, instead, uses two adjacent test cells to pass current through the coating [43, 44]. The test set-up uses the following three electrodes:

- WE – A platinum mesh or other conductive and inert material with a large surface area and high current density.
- CE – A platinum mesh or similar as for the WE.
- RE – Field grade CSE (preferably pencil style), SSCE, or SCE. If necessary, a conductive, inert material is suitable.

4.2.1. Materials

Table 4 provides a list of field EIS equipment items for a single, no connection to substrate test. The test requires two 100-milliliter (mL) plastic beakers, or similar, to provide the physical test cell when glued to the coating surface via marine adhesive. Gluing extra test cell allows for more data or substitutes for cells with inadequate adhesion. A CSE provides the RE and two platinum mesh electrodes in separate test cells provide the CE and WE. The rubber stopper fixture suspends the RE and CE in one test cell via penetrations. Electrolyte for the test cell reduces the resistance between the electrodes and the coating surface. Tap water provides a field-ready electrolyte option. Treatment with an estimated 1 tablespoon of table salt (approximately 20 grams of NaCl) per liter further decreases its resistance. Other electrolytes such as conductive gels are suitable [17, 34].

Table 4. Equipment items for one field EIS test cell setup

• Portable potentiostat	• 100-mL beaker (2) (bottom removed)	• Copper-copper sulfate electrode (RE)
• Laptop computer/processor	• Marine adhesive	• Platinum mesh (2) (CE & WE)
• Electrolyte & reservoir	• Rubber stopper fixture	

4.2.1. Method

Below is a step-by-step method for performing field EIS inspections on coated structures. It includes footnotes to further describe pertinent items or provide the user with additional information.

Provided below is a test method for coated infrastructure. The method measures the coating's dielectric properties. The data indicates the extent of coating degradation at the time of the test. Initiate Step 1 prior to arriving on site.

1. Determine coating type and age. Consult project specifications, submittals, and facility personnel for information. Identify a sampling approach to collect more than 30 data sets, commensurate with the drivers presented in Section 3.1. Coating Sampling (Estimating Coating Quality). Prepare test beakers by cutting off or otherwise removing the bottom. Ensure there are enough beakers for each proposed test site. Determine the number of shifts or days required and draft an inspection schedule.⁴
2. Select undamaged coating as test cell site. Remove mud and dirt from coating surface with a wet rag and wipe dry with a clean rag. Inspect surface for cracks, rust-through, or other defects to ensure there are no visible coating flaws within the test cell. Apply adhesive to the rim of the 100-mL beaker and place against the coating surface to encourage a good bond and full seal (Figure 15).⁵
3. Add tap water or prepared electrolyte solution to test cell after glue cures sufficiently to hold its seal. Allow electrolyte to saturate into coating to achieve equilibrium.⁶
4. Complete test cell setup by placing the WE in one cell and the RE / CE rubber stopper combination in the second test cell (Figure 16). Prepare the potentiostat software using recommended test parameters (Table 5) with adjustments as needed and begin the test.⁷
5. Begin experiment and monitor the OCP measurement to ensure the system is at steady state, i.e., the OCP is not increasing or decreasing systematically. An acceptable allowance for potential drift is ± 1.0 mV per 30 sec. Stop the experiment if not stable and ensure that instrument wire lead connections are correct and secure.⁸

⁴ Perform tasks as a job planning phase prior to arriving on site. Treat coating areas with different materials or exposure conditions as a separate data set. EIS testing on spot repairs is lower priority, and testing efforts should be proportional to the percentage of the structure containing these repairs.

⁵ Lower pipe walls or other horizontal surfaces are the easiest application for field EIS testing. Pipe interiors often contain source water in the invert for cleaning the coating surface. Avoid placing test cells on rough or textured coating surfaces to ensure a good seal. A fast-curing aquarium-grade silicone cures within 30 minutes at approximately 70 degrees Fahrenheit.

⁶ Equilibration time is less than 15 minutes if structure unwatering occurred same day. Completely dry coatings or excellent barriers with minimal degradation may require a full day (overnight) to saturate.

⁷ For Ivium Compactstat 10800, connect potentiostat to laptop via USB port. Open potentiostat software and click Connect. Wait for a series of two beeps to indicate potentiostat connection is live. Select Potentiostatic EIS test template. The test duration is approximately two to three minutes for the given parameters. Reducing the End Frequency or increasing the points per decade provides additional data at the expense of test duration.

⁸ The field EIS setup does not use a Faraday cage, but a pipe interior generally provides a low electrochemical noise environment. Ensure all cellular emitting devices are in airplane mode or off and reduce use of transmitting equipment to maximize data quality. Structure polarization could also affect this ungrounded experiment.

6. Ensure the test finishes, the data set is reasonable, and the data file saves to the intended location. Repeat if uncertain then move to the next location.



Figure 15. Attachment of EIS test cells to clean, dry, and defect-free coating surface.

Table 5. Recommended field EIS parameters and inputs.

Parameter	Input
Open Circuit Potential (OCP)	15 seconds (sec)
Start Frequency	10^5 Hz
End Frequency	10^{-1} Hz
Voltage Amplitude	50 mV
Points per Decade	5

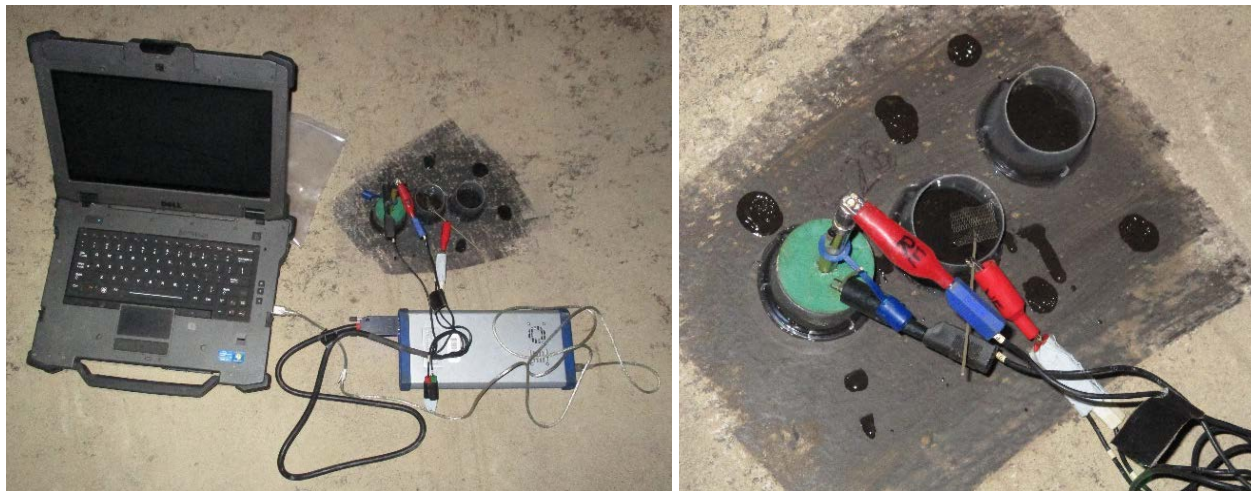


Figure 16. Field EIS test (left) overview of setup and (right) detail of test cells and electrodes.

5. References

- [1] Bacon, R. C., Smith, J. J., and Rugg, F. M., "Electrolytic Resistance in Evaluating Protective Merit of Coatings on Metals," *Industrial & Engineering Chemistry*, Vol. 40, No. 1, 1948, p. 161, <http://dx.doi.org/10.1021/ie50457a041>.
- [2] Kendig, M., and Mills, D. J., "An historical perspective on the corrosion protection by paints," *Progress in Organic Coatings*, Vol. 102, Part A, 2017, p. 53, <http://dx.doi.org/https://doi.org/10.1016/j.porgcoat.2016.04.044>.
- [3] Loveday, D., Peterson, P., and Rodgers, B., "Evaluation of organic coatings with electrochemical Impedance Spectroscopy Part 1: Fundamentals of electrochemical impedance spectroscopy," *JCT Coatings Tech*, Vol. 1, No. August, 2004, p. 46.
- [4] Loveday, D., Peterson, P., and Rodgers, B., "Evaluation of organic coatings with electrochemical impedance spectroscopy Part 2: Application of EIS to coatings," *JCT Coatings Tech*, Vol. 1, 2004, p. 88.
- [5] Loveday, D., Peterson, P., and Rodgers, B., "Evaluation of organic coatings with electrochemical impedance spectroscopy Part 3: Protocols for testing coatings with EIS," *JCT Coatings Tech*, Vol. 2, 2005, p. 22.
- [6] Scully, J. R., "Electrochemical Impedance of Organic-Coated Steel: Correlation of Impedance Parameters with Long-Term Coating Deterioration," *Journal of the Electrochemical Society*, Vol. 136, No. 4, 1989, p. 979, <http://dx.doi.org/10.1149/1.2096897>.
- [7] Scully, J. R., and Hensley, S. T., "Lifetime Prediction for Organic Coatings on Steel and a Magnesium Alloy Using Electrochemical Impedance Methods," *CORROSION*, Vol. 50, No. 9, 1994, p. 705, <http://dx.doi.org/10.5006/1.3293547>.
- [8] Bierwagen, G., Tallman, D., Li, J., Hea, L., and Jeffcoate, C., "EIS studies of coated metals in accelerated exposure," *Progress in Organic Coatings*, Vol. 46, 2003, p. 148.
- [9] Kendig, M., Mansfeld, F., and Tsai, S., "Determination of the long term corrosion behavior of coated steel with A.C. impedance measurements," *Corrosion Science*, Vol. 23, No. 4, 1983, p. 317, [http://dx.doi.org/https://doi.org/10.1016/0010-938X\(83\)90064-1](http://dx.doi.org/https://doi.org/10.1016/0010-938X(83)90064-1).

- [10] Hinderliter, B. R., Croll, S. G., Tallman, D. E., Su, Q., and Bierwagen, G. P., "Interpretation of EIS data from accelerated exposure of coated metals based on modeling of coating physical properties," *Electrochimica Acta*, Vol. 51, No. 21, 2006, p. 4505, <http://dx.doi.org/https://doi.org/10.1016/j.electacta.2005.12.047>.
- [11] Lvovich, V. F., *Impedance Spectroscopy: Applications to Electrochemical and Dielectric Phenomena*, John Wiley & Sons, Hoboken, N.J., 2012.
- [12] Wolstenholme, J., "Electrochemical methods of assessing the corrosion of painted metals—a review," *Corrosion Science*, Vol. 13, No. 7, 1973, p. 521, [http://dx.doi.org/https://doi.org/10.1016/S0010-938X\(73\)80002-2](http://dx.doi.org/https://doi.org/10.1016/S0010-938X(73)80002-2).
- [13] "ASTM G106-89(2015), Standard Practice for Verification of Algorithm and Equipment for Electrochemical Impedance Measurements," ASTM International, 2015.
- [14] Tsai, C. H., and Mansfeld, F., "Determination of Coating Deterioration with EIS: Part II. Development of a Method for Field Testing of Protective Coatings," *CORROSION*, Vol. 49, No. 9, 1993, p. 726, <http://dx.doi.org/10.5006/1.3316106>.
- [15] Papavinasam, S., Attard, M., and Revie, R. W., "Electrochemical Impedance Spectroscopy Measurement During Cathodic Disbondment Experiment of Pipeline Coatings," *Journal of ASTM International*, Vol. 6, No. 3, 2009, p. 1, <http://dx.doi.org/10.1520/JAI101246>.
- [16] Merten, B. J., Skaja, A., Tordonato, D., and Little, D., "Re-evaluating Electrochemical Impedance Spectroscopy (EIS) for the Field Inspector's Toolbox: A First Approach," SSPC 2014, SSPC: The Society for Protective Coatings.
- [17] Gray, L. G. S., and Appleman, B. R., "EIS: Electrochemical Impedance Spectroscopy," *Journal of Protective Coatings & Linings*, Vol. 20, No. 2, 2003.
- [18] Bordziłowski, J., Królikowska, A., Bonora, P. L., Maconi, I., and Sollichc, A., "Underwater EIS measurements," *Progress in Organic Coatings*, Vol. 67, 2010, p. 414.
- [19] Sonke, J., and Consultancy, S., "Qualification of Protective Coatings using EIS," presented at *EUROCORR 2008*, Edinburgh, Scotland, 7-11 September 2008.
- [20] Jones, D. A., *Principles and Prevention of Corrosion*, 2nd ed., Prentice Hall, Upper Saddle River, NJ, 1996, p. 109-113.

[21] Kelly, R. G., Scully, J. R., Shoesmith, D., and Buchheit, R. G., *Electrochemical Techniques in Corrosion Science and Engineering*, CRC Press, 2002, p. Chapter 4.

[22] Mansfeld, F., and Tsai, C. H., "Determination of Coating Deterioration with EIS: I. Basic Relationships," *CORROSION*, Vol. 47, No. 12, 1991, p. 958, <http://dx.doi.org/10.5006/1.3585209>.

[23] Kendig, M. W., Jeanjaquet, S., and Lumsden, J., "Electrochemical Impedance of Coated Metal Undergoing Loss of Adhesion," *Electrochemical Impedance: Analysis and Interpretation*, ASTM STP18082S, J. R. Scully, D. C. Silverman, and M. W. Kendig Eds. ASTM International, West Conshohocken, PA, 1993, p. 407, <http://dx.doi.org/10.1520/STP18082S>.

[24] Hirayama, R., and Haruyama, S., "Electrochemical Impedance for Degraded Coated Steel Having Pores," *CORROSION*, Vol. 47, No. 12, 1991, p. 952, <http://dx.doi.org/10.5006/1.3585208>.

[25] Brasher, D. M., and Kingsbury, A. H., "Electrical measurements in the study of immersed paint coatings on metal. I. Comparison between capacitance and gravimetric methods of estimating water-uptake," *Journal of Applied Chemistry*, Vol. 4, No. 2, 1954, p. 62, <http://dx.doi.org/10.1002/jctb.5010040202>.

[26] Nguyen, A. S., Causse, N., Musiani, M., Orazem, M. E., Pébère, N., Tribollet, B., and Vivier, V., "Determination of water uptake in organic coatings deposited on 2024 aluminium alloy: Comparison between impedance measurements and gravimetry," *Progress in Organic Coatings*, Vol. 112, 2017, p. 93, <http://dx.doi.org/https://doi.org/10.1016/j.porgcoat.2017.07.004>.

[27] Vosgien Lacombe, C., Bouvet, G., Trinh, D., Mallarino, S., and Touzain, S., "Water uptake in free films and coatings using the Brasher and Kingsbury equation: a possible explanation of the different values obtained by electrochemical Impedance spectroscopy and gravimetry," *Electrochimica Acta*, Vol. 231, 2017, p. 162, <http://dx.doi.org/https://doi.org/10.1016/j.electacta.2017.02.051>.

[28] Lyon, S. B., Bingham, R., and Mills, D. J., "Advances in corrosion protection by organic coatings: What we know and what we would like to know," *Progress in Organic Coatings*, Vol. 102, Part A, 2017, p. 2, <http://dx.doi.org/https://doi.org/10.1016/j.porgcoat.2016.04.030>.

[29] Mills, D., and Mayne., J., "Inhomogeneous Nature of Polymer Films and Its Effect on Resistance Inhibition," *Corrosion Control by Organic Coatings*, H. Leidheiser Eds. NACE International, Houston, TX, 1981, p. 12.

[30] Mills, D. J., and Jamali, S. S., "The best tests for anti-corrosive paints. And why: A personal viewpoint," *Progress in Organic Coatings*, Vol. 102, Part A, 2017, p. 8, <http://dx.doi.org/https://doi.org/10.1016/j.porgcoat.2016.04.045>.

[31] Merten, B. J. E., Prochaska, S. O., and Tordonato, D. S., Pittsburgh, PA, "Comparison of Field Impedance Measurements to Laboratory Data," Orlando, FL, 2019.

[32] Merten, B. J. E., Walsh, M. T., and Torrey, J. D., "Validation of Coated Infrastructure Examination by Electrochemical Impedance Spectroscopy," *Advances in Electrochemical Techniques for Corrosion Monitoring and Laboratory Corrosion Measurements, ASTM STP1609*, S. Papavinasam, R. B. Rebak, L. Yang, and N. S. Berke Eds. ASTM International, West Conshohocken, PA, 2019.

[33] Bureau of Reclamation, "The 10% Soil Resistivity Method," MERL-05-19, U.S. Department of the Interior, Bureau of Reclamation, Denver, CO, 2005.

[34] Bortak, T., "Evaluation and Remaining Service Life of Protective Coatings by Electrochemical Impedance Spectroscopy (EIS)," MERL-04-09, September 2004.

[35] Martin, J. W., *Methodologies For Predicting The Service Lives Of Coating Systems*, Vol. Nist Building Science Series 172, U.S. Department Of Commerce, National Institute of Standards Technology, 1994.

[36] Shreepathi, S., Guin, A. K., Naik, S. M., and Vattipalli, M. R., "Service life prediction of organic coatings: electrochemical impedance spectroscopy vs actual service life," *Journal of Coatings Technology and Research*, Vol. 8, No. 2, 2011, p. 191, <http://dx.doi.org/10.1007/s11998-010-9299-5>.

[37] Kendig, M., and Scully, J., "Basic Aspects of Electrochemical Impedance Application for the Life Prediction of Organic Coatings on Metals," *CORROSION*, Vol. 46, No. 1, 1990, p. 22, <http://dx.doi.org/10.5006/1.3585061>.

[38] Thu, Q. L., Bierwagen, G. P., and Touzain, S., "EIS and ENM measurements for three different organic coatings on aluminum," *Progress in Organic Coatings*, Vol. 42, 2001, p. 179.

[39] *Impedance Spectroscopy: Theory, Experiment, and Applications*, 3rd ed., John Wiley & Sons, Inc., Hoboken, NJ, 2018.

[40] Mansfeld, F., Shih, H., Greene, H., and Tsai, C. H., *Analysis of EIS data for common corrosion processes*, ASTM, Philadelphia, PA, 1993.

[41] Randles, J. E. B., "Kinetics of rapid electrode reactions," *Discussions of the Faraday Society*, Vol. 1, No. 0, 1947, p. 11, <http://dx.doi.org/10.1039/DF9470100011>.

[42] Touzain, S., "Some comments on the use of the EIS phase angle to evaluate organic coating degradation," *Electrochimica Acta*, Vol. 55, 2010, p. 6190, <http://dx.doi.org/10.1016/j.electacta.2009.09.045>.

[43] Allahar, K., Su, Q., and Bierwagen, G., "Non-substrate EIS monitoring of organic coatings with embedded electrodes," *Progress in Organic Coatings*, Vol. 67, No. 2, 2010, p. 180, <http://dx.doi.org/10.1016/j.porgcoat.2009.10.001>.

[44] Mills, D., Picton, P., and Mularczyk, L., "Developments in the electrochemical noise method (ENM) to make it more practical for assessment of anti-corrosive coatings," *Electrochimica Acta*, Vol. 124, 2014, p. 199, <http://dx.doi.org/https://doi.org/10.1016/j.electacta.2013.09.067>.

